

A new scheme developed for the numerical simulation of the Boltzmann equation using the direct simulation monte-carlo scheme for the flow about a sphere

S. S. Nourazar* and A. A. Ganjaei

Mechanical Engineering Department, Amirkabir University of Technology, Tehran, Iran

(Manuscript Received June 29, 2009; Revised May 9, 2010; Accepted June 5, 2010)

Abstract

A new scheme, the modified direct simulation Monte-Carlo (MDSMC), for the numerical simulation of the Boltzmann equation for rarefied gas flow about a sphere is developed. The Taylor series expansion is used to obtain the modified equation of the first-order time discretization of the collision equation and the new scheme, MDSMC, is implemented to simulate the collision equation in the Boltzmann equation. In the new scheme (MDSMC) there exists a new extra term which takes into account the effect of the second-order collision. In the new scheme (MDSMC) there also exists a second-order term in time step in the probabilistic coefficients which has the effect of simulation with higher accuracy than the previous DSMC scheme. The results of the drag coefficient of the sphere using the MDSMC scheme show better agreement in comparison with the experimental data of Wegener (1961) than the results of the drag coefficient of the sphere using the DSMC scheme.

Keywords: Boltzmann equation; DSMC; External flow; High order DSMC; Modified DSMC; Rarefied gas flow

1. Introduction

In gas flow problems where the length scale of the system is comparable to the mean free path for molecules in the gas flow, the concept of the continuum is no more valid, Knudsen number greater than 0.1, (Bird, 1994). In this case, the simulation is done using the collisional Boltzmann equation (CBE) methods. In most cases, the direct solution of the CBE is impracticable due to the huge number of molecules; however, most of the time the implementation of the DSMC is more practicable. The Boltzmann equation was derived by Ludwig Eduard Boltzmann in 1872, and the limited conditions was studied by Cercignani (1969). So far the rarefied gas flow problems about a blunt body are simulated using the DSMC scheme by Vogenitz, et al. (1968), Bird (1994), Garcia, et al.(1997), Crifo, et al. (2002), Chen, et al.(2003), Wu, et al.(2003), Volkov, et al. (2005) and Nourazar, et al. (2005). The DSMC scheme is used in the flow simulation of the previous researchers and the results of the simulations show some discrepancies when compared with the experimental data.

The external rarefied gas flow about the blunt body is simulated. Vogenitz, et al. (1968) studied the theoretical and experimental aspects of the rarefied supersonic flow about sev-

eral simple shapes (sphere, cylinder, cone and wedge). Their results of simulation show less discrepancy at high Knudsen number than low Knudsen number when compared with measurements. The results of the external gas flow using DSMC scheme are presented in Bird's book. Bird studied rarefied gas flow over the flat nose cylinder and presented the results of this simulation in his book. But, Bird didn't compare the results of the external rarefied gas flow using DSMC with the experimental data. Crifo, et al. (2002) compared between Navier Stokes and Boltzmann simulation of the circumnuclear coma. They considered perfect agreement between the two methods on the day and night sides of the coma. Chen, et al. (2003) extended the Boltzmann kinetic equation for turbulent flows. In their work, it is shown the effectiveness of the method with the use of a computationally efficient implementation in terms of a lattice Boltzmann equation. Wu, et al. (2003) used the parallel three-dimensional direct simulation Monte-Carlo methods for simulation of a hypersonic flow about a sphere. They compared their results with Dogra, et al.'s (1994) results. This comparison shows a good agreement between two results. Volkov, et al. (2005) simulated a supersonic multiphase gas solid flow over a blunt body. The carrier gas is treated as a continuum and described by the complete Navier Stokes equations with additional source terms modeling the reverse action of the dispersed phase; the dispersed phase is treated as a discrete set of solid particles and its behavior is described by a kinetic Boltzmann equation.

† This paper was recommended for publication in revised form by Associate Editor Man-Yeong Ha

*Corresponding author. Tel.: +82 55 751 6106, Fax: +82 55 757 5622

E-mail address: icp@aut.ac.ir

© KSME & Springer 2010

In this study, we would like to develop a scheme to simulate the collision equation in the Boltzmann equation with higher accuracy than the previous schemes available in the literature and apply this scheme to solve the external flow about the sphere.

1.1 Purpose of the present work

So far the rarefied gas dynamic problems, when the Knudsen number is large enough, are simulated using the first-order time discretization of the Boltzmann equation (Bird, 1994). The Boltzmann equation is split in time into a purely convective equation (collision term is zero) and a purely collision equation (convective term is zero). The collision equation is discretized in time by the first-order Euler scheme, and the probabilistic interpretation of the discretized equation breaks down when the ratio $\mu\Delta t/\varepsilon$ is large enough (Nanbu (1980), Babovsky (1986) and Pareschi (2005)). However, in the present work our goal is to develop a scheme which considers the effects of the truncation errors in the time discretization of the first-order Euler scheme for the collision equation in order to achieve more accurate probabilistic interpretations. To achieve this goal, we write the modified equation of the first-order Euler scheme using the Taylor expansion series and then we capture the higher order truncated terms. In the present work due to the limitation of the computing time we are limited to choosing only the first two terms in the Taylor expansion series. The details of the derivation of our scheme which we call that modified direct simulation Monte-Carlo (MDSMC) scheme are presented in the §2b the MDSMC scheme.

1.2 Description of case study problems

To validate our scheme we consider the external rarefied gas flow about a sphere as our case study problem with the data exactly the same as one depicted by the experiment of Wegener, et al. (1961). In the case study, the drag coefficient for a sphere in the external rarefied gas flow is simulated using the MDSMC and DSMC schemes and the results of the simulation are compared with the experimental data of Wegener, et al. (1961). The diameter of the sphere is 12.7 mm (0.5 in) and the fluid flowing about the sphere is chosen to be air. Six different ambient temperatures, ambient Mach numbers and ambient Knudsen numbers are chosen to be the same as the experimental data of Wegener, et al. (1961). The numerical values of the temperatures, Mach numbers and Knudsen numbers are given in Table 1.

The schematic diagram of our case study problem is shown in Fig. 1.

1.3 Boundary conditions

The sizes of calculation domain are, $L_x=25.7$ mm, $L_y=12.7$ mm and the diameter of the sphere= 12.7 mm. The number of cells in X direction is 400. The number of cells in Y direction is 200. The total number of cells is 80000. The velocities of

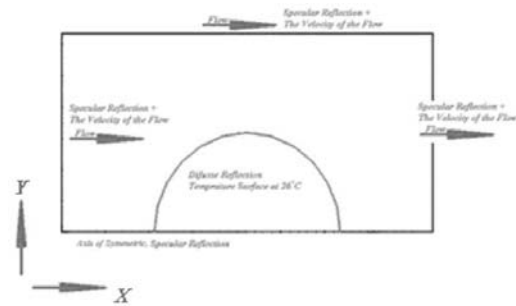


Fig. 1. The schematic diagram of the case study in the present work.

flow, in Fig. 1, are 1482.37335 m/s, 1498.6708 m/s, 1389.6773 m/s, 1420.5436 m/s, 1390.373 m/s and 1446.585 m/s.

1.4 Parameters of VHS model

The reference of diameter of air molecules is 4.19×10^{-10} m. The reference temperature of air molecules is 273K. The viscosity temperature power law is 0.746. The molecular mass of air molecules is 47.82×10^{-27} Kg. The number of rotational degree of freedom of air molecules is 5.

2. Mathematical formulations

2.1 The Boltzmann equation

The Boltzmann equation is written as (Cercignani, 1988):

$$\frac{\partial f}{\partial t} + \mathbf{v} \cdot \nabla_r f = \frac{1}{\varepsilon} \int \int \int \sigma(|\mathbf{v} - \mathbf{v}_*|, \Omega) \begin{pmatrix} f(\mathbf{v}') f(\mathbf{v}_*') \\ -f(\mathbf{v}) f(\mathbf{v}_*) \end{pmatrix} d\Omega d\mathbf{v}_* . \quad (1)$$

$$= \frac{1}{\varepsilon} Q(f, f)$$

In Eq. (1), $f(\mathbf{v})$ is the nonnegative density probability distribution function of molecule of class having the velocity of \mathbf{v} , $f(\mathbf{v}_*)$ is the nonnegative density probability distribution function of the molecule of class having the velocity of \mathbf{v}_* , $f(\mathbf{v}')$ is the post-collision nonnegative density probability distribution function of the molecule of class having the velocity of \mathbf{v}' , and $f(\mathbf{v}_*')$ is the post-collision nonnegative density probability distribution function of the molecule of class having the velocity of \mathbf{v}_*' and Ω is the angle in the spherical coordinates. The $Q(f, f)$ is the integral collision which describes the binary collisions of the molecules. The kernel σ is a non-negative function which is described as (Pareschi, 2005):

$$\sigma(|\mathbf{v} - \mathbf{v}_*|, \Omega) = b_\alpha(\theta) |\mathbf{v} - \mathbf{v}_*|^\alpha . \quad (2)$$

Where, θ is the scattering angle between $\mathbf{v} - \mathbf{v}_*$ and $|\mathbf{v} - \mathbf{v}_*| \Omega$. The variable hard sphere (VHS) (Bird, 1994)

model is often used in numerical simulation of rarefied gases, where, $b_\alpha(\theta) = C$ with C a positive constant and $\alpha = 1$. The value of C is equal to (Bird, 1994), $C = \sigma_T$, where σ_T is the collision cross section and is equal to $\pi d^2/4$.

2.2 The MDSMC scheme

Splitting Eq. (1), the Boltzmann equation (Gabetta, et al., 1997), into an equation for the effect of collision, $\mathbf{v} \cdot \nabla_r f \equiv 0$, and an equation for the effect of convection, $Q(f, f) \equiv 0$. The equation for the effect of convection is written as (Pareschi, 2005):

$$\frac{\partial f}{\partial t} + \mathbf{v} \cdot \nabla_r f = 0. \tag{3}$$

The equation for the effect of collision is written as (Pareschi, 2005):

$$\frac{\partial f}{\partial t} = \frac{1}{\varepsilon} Q(f, f), \tag{4}$$

where the right hand side of Eq. (4) is called the collision term and is rewritten as:

$$\begin{aligned} \frac{1}{\varepsilon} Q(f, f) &= \int_{-\infty}^{+\infty} \int_0^{4\pi} \sigma_T |\mathbf{v} - \mathbf{v}_*| [f(\mathbf{v}') f(\mathbf{v}'_*) - f(\mathbf{v}) f(\mathbf{v}_*)] d\Omega dv_* \\ &= \int_{-\infty}^{+\infty} \int_0^{4\pi} \sigma_T |\mathbf{v} - \mathbf{v}_*| f(\mathbf{v}') f(\mathbf{v}'_*) d\Omega dv_* \\ &\quad - f(\mathbf{v}) \int_{-\infty}^{+\infty} \int_0^{4\pi} \sigma_T |\mathbf{v} - \mathbf{v}_*| f(\mathbf{v}_*) d\Omega dv_* \\ &= \frac{1}{\varepsilon} [P(f, f) - \mu(\mathbf{v}) f]. \end{aligned} \tag{5}$$

Where,

$$\begin{aligned} \mu(\mathbf{v}) &= \int_{-\infty}^{+\infty} \int_0^{4\pi} \sigma_T |\mathbf{v} - \mathbf{v}_*| f(\mathbf{v}_*) d\Omega dv_* = \int_{-\infty}^{+\infty} \sigma_T |\mathbf{v} - \mathbf{v}_*| d\Omega \\ \int_0^{4\pi} f(\mathbf{v}_*) dv_* &= \kappa \rho / m \text{ is the mean collision frequency for the molecules having velocity } \mathbf{v}, \rho \text{ is the density of the gas, } m \text{ is the mass of a molecule of the gas, } \kappa \text{ is a molecular constant} \\ \kappa &= \int_0^{4\pi} \sigma_T |\mathbf{v} - \mathbf{v}_*| d\Omega \text{ and } \rho / m = \int_{-\infty}^{+\infty} f(\mathbf{v}_*) dv_* \text{ (Wild, 1951):} \end{aligned}$$

$$\mu(\mathbf{v}) = \mu = \frac{\kappa \rho}{m}. \tag{6}$$

Substituting Eq. (6) into Eq. (5) and then into Eq. (4):

$$\frac{\partial f}{\partial t} = \frac{1}{\varepsilon} Q(f, f) = \frac{1}{\varepsilon} [P(f, f) - \mu f]. \tag{7}$$

The first-order time discretization of Eq. (7) is written as:

$$f^{n+1} = \left(1 - \frac{\mu \Delta t}{\varepsilon}\right) f^n + \frac{\mu \Delta t}{\varepsilon} \frac{P(f^n, f^n)}{\mu}. \tag{8}$$

The probabilistic interpretation of Eq. (7) is the following. In order a particle is sampled from f^{n+1} , a particle is sampled from f^n with probability of $(1 - \mu \Delta t / \varepsilon)$ and a particle is sampled from $P(f^n, f^n) / \mu$ with probability of $\mu \Delta t / \varepsilon$. It is to be noted that the above probabilistic interpretation fails if the ratio of $\mu \Delta t / \varepsilon$ is too large because the coefficient of f^n on the right hand side may become negative (Nanbu, 1980, Babovsky, 1986 and Pareschi, 2005).

In our scheme, we write for f^{n+1} from Taylor series expansion as:

$$\begin{aligned} f^{n+1} &= f^n + \Delta t \left. \frac{\partial f}{\partial t} \right|^n \\ &\quad + \frac{(\Delta t)^2}{2!} \left. \frac{\partial^2 f}{\partial t^2} \right|^n + O(\Delta t)^3. \end{aligned} \tag{9}$$

The second-order derivative, $\partial^2 f / \partial t^2$, in Eq. (9) is written as:

$$\begin{aligned} \left. \frac{\partial^2 f}{\partial t^2} \right|^n &= \frac{\partial}{\partial t} \left(\left. \frac{\partial f}{\partial t} \right|^n \right) \\ &= \frac{\partial}{\partial t} \left(\frac{1}{\varepsilon} [P(f^n, f^n) - \mu f^n] \right)^n \\ &= \frac{1}{\varepsilon} \frac{\partial P(f^n, f^n)}{\partial t} - \frac{\mu}{\varepsilon} \left. \frac{\partial f^n}{\partial t} \right|^n \\ &= \frac{1}{\varepsilon} \frac{\partial P(f^n, f^n)}{\partial t} - \frac{\mu}{\varepsilon} \left(\frac{1}{\varepsilon} [P(f^n, f^n) - \mu f^n] \right) \\ &= \frac{1}{\varepsilon} \frac{\partial P(f^n, f^n)}{\partial t} - \frac{\mu}{\varepsilon^2} P(f^n, f^n) + \frac{\mu^2}{\varepsilon^2} f^n. \end{aligned} \tag{10}$$

Substituting Eq. (10) for the value of $\partial^2 f / \partial t^2$ and Eq. (7) for the value of $\partial f / \partial t$ into Eq. (9):

$$\begin{aligned} f^{n+1} &= f^n + \frac{\Delta t}{\varepsilon} [P(f^n, f^n) - \mu f^n] + \\ &\quad \frac{(\Delta t)^2}{2!} \left(\frac{1}{\varepsilon} \frac{\partial P(f^n, f^n)}{\partial t} - \frac{\mu}{\varepsilon^2} P(f^n, f^n) + \frac{\mu^2}{\varepsilon^2} f^n \right) \\ &\quad + O(\Delta t)^3. \end{aligned} \tag{11}$$

The $P(f^n, f^n) = \int_{-\infty}^{+\infty} \int_0^{4\pi} \sigma_T |\mathbf{v} - \mathbf{v}_*| f^n(\mathbf{v}') f^n(\mathbf{v}'_*) d\Omega dv_*$ is the bilinear operator describing the collision effect of two molecules. The time derivative of $P(f^n, f^n)$ is rewritten as:

$$\begin{aligned} \frac{\partial P(f^n, f^n)}{\partial t} &= \int_{-\infty}^{+\infty} \int_0^{4\pi} \sigma_T |\mathbf{v} - \mathbf{v}_*| \frac{\partial f^n(\mathbf{v}')}{\partial t} f^n(\mathbf{v}'_*) d\Omega dv_*. \end{aligned} \tag{12}$$

The time discretization of $\partial P(f^n, f^n)/\partial t$ is rewritten as:

$$\begin{aligned} \frac{\partial P(f^n, f^n)}{\partial t} &= \\ & \int_{-\infty}^{+\infty} \int_0^{4\pi} \sigma_T |\mathbf{v} - \mathbf{v}_*| \left(\frac{f_i^n(\mathbf{v}') - f^n(\mathbf{v}')}{\Delta t} \right) f(\mathbf{v}_*) d\Omega dv_* \\ &= \frac{1}{\Delta t} \left\{ \int_{-\infty}^{+\infty} \int_0^{4\pi} \sigma_T |\mathbf{v} - \mathbf{v}_*| f_i^n(\mathbf{v}') f(\mathbf{v}_*) d\Omega dv_* \right. \\ & \quad \left. - \int_{-\infty}^{+\infty} \int_0^{4\pi} \sigma_T |\mathbf{v} - \mathbf{v}_*| f^n(\mathbf{v}') f(\mathbf{v}_*) d\Omega dv_* \right\}. \end{aligned} \quad (13)$$

Substituting for

$$P(f^n, f^n) = \int_{-\infty}^{+\infty} \int_0^{4\pi} \sigma_T |\mathbf{v} - \mathbf{v}_*| f^n(\mathbf{v}') f(\mathbf{v}_*) d\Omega dv_*$$

into Eq. (13):

$$\begin{aligned} \frac{\partial P(f^n, f^n)}{\partial t} &= \\ & \frac{1}{\Delta t} \{ P(f_1^n, f^n) - P(f^n, f^n) \}. \end{aligned} \quad (14)$$

Substituting Eq. (14) into Eq. (11):

$$\begin{aligned} f^{n+1} &= f^n \\ &+ \frac{\mu \Delta t}{\varepsilon} \left[\frac{P(f_1^n, f^n)}{\mu} - f^n \right] \\ &+ \frac{(\Delta t)^2}{2!} \left(\frac{\mu}{\varepsilon \Delta t} \left[\frac{P(f^n, f^n)}{\mu} - \frac{P(f_1^n, f^n)}{\mu} \right] \right. \\ & \quad \left. - \frac{\mu^2}{\varepsilon^2} \frac{P(f^n, f^n)}{\mu} + \frac{\mu^2}{\varepsilon^2} f^n \right) \\ &+ O(\Delta t)^3, \end{aligned} \quad (15)$$

where $f_i^n = P(f^n, f^n)/\mu$. Rearranging and truncating terms of higher order than the second order in Eq. (15):

$$\begin{aligned} f^{n+1} &= \left(1 - \frac{\mu \Delta t}{\varepsilon} + \frac{\mu^2 (\Delta t)^2}{2\varepsilon^2} \right) f^n \\ &+ \left(\frac{\mu \Delta t}{2\varepsilon} - \frac{\mu^2 (\Delta t)^2}{2\varepsilon^2} \right) \frac{P(f^n, f^n)}{\mu} \\ &+ \frac{\mu \Delta t}{2\varepsilon} \frac{P(f_1^n, f^n)}{\mu}. \end{aligned} \quad (16)$$

The probabilistic interpretation of Eq. (16) is the following. In order a particle is sampled from f^{n+1} , a particle is sampled from f^n with probability of $(1 - \mu \Delta t / \varepsilon + \mu^2 (\Delta t)^2 / 2\varepsilon^2)$, a particle is sampled from $P(f^n, f^n)/\mu$ with probability of $(\mu \Delta t / 2\varepsilon - \mu^2 (\Delta t)^2 / 2\varepsilon^2)$ and a particle is sampled from $P(f_1^n, f^n)/\mu$ with probability of $\mu \Delta t / 2\varepsilon$. Comparing Eq.

(16), the new scheme (MDSMC), with Eq. (8) (the DSMC scheme) reveals two facts as follows: 1- Eq. (16), the new scheme (MDSMC), consists of three terms that are sampled probabilistically; however, Eq. (8) (the DSMC scheme) consists of two terms that are sampled probabilistically, the third extra term in Eq. (16), $P(f_1^n, f^n)/\mu$, is interpreted as the collision between the particles sampled from f^n and the particles sampled from $P(f^n, f^n)/\mu$. 2- The probabilistic coefficients in Eq. (16), the new scheme (MDSMC), consist of the second-order terms in time step; however, the probabilistic coefficients in Eq. (8) (the DSMC scheme) consist of the first-order terms in the time step.

3. The drag coefficient calculation

In this paper, the drag coefficient of the sphere is calculated simulating the flow field using the DSMC and the MDSMC schemes. Then the results of the simulation are compared with Wegener's experimental data for the drag coefficient of the sphere in the low-pressure tunnel. The drag force acting on the sphere is written as:

$$f_{drag} = \int_0^{\pi} \int_0^{2\pi} r^2 \sigma_{rr} \cos\theta \sin\phi d\phi d\theta. \quad (17)$$

The drag coefficient is defined as:

$$C_D = \frac{f_{drag}}{1/2 \rho V^2 A_s}, \quad (18)$$

where the A_s is the cross section of the sphere, $A_s = \pi/4 d_s^2$, and d_s is the diameter of the sphere.

4. The numerical procedures

4.1 The DSMC scheme (the VHS collision model molecules):

- $\Delta t = 0.5 \times 10^{-8}$ Sec
- Distribute the initial locations of the particles according to the uniform distribution.
 - Given $\{ \mathbf{x}_i^n, i = 1, \dots, N \}$ and $\{ \mathbf{v}_i^n, i = 1, \dots, N \}$
 - Set $\mathbf{x}_i^{n+1} = \mathbf{x}_i^n + \mathbf{v}_i^n \cdot \Delta t$
- for $n_i = 1$ to n_{tot}
 - Given $\{ \mathbf{v}_i^n, i = 1, \dots, N \}$.
 - Define the local Knudsen number (ε).
- Compute an upper bound $\bar{\sigma} = \max [(\pi d^2 |\mathbf{v}_i - \mathbf{v}_j|) / 4]$ for the cross section, $\bar{\sigma}$ is updated in each collision.
- Set $\mu = 4\pi \bar{\sigma}$.
- Set $N_c = Iround(\mu N \Delta t / (2\varepsilon))$.
- Select $2N_c$ dummy collision pairs (i, j) uniformly among all possible pairs, and for those.
- Compute the relative cross section $\sigma_{ij} = \pi d^2 |\mathbf{v}_i - \mathbf{v}_j| / 4$.
- Generate uniform random numbers $Rand$.
- If $Rand < \sigma_{ij} / \bar{\sigma}$

- Perform the collision between i and j , and compute the post-collision velocities \mathbf{v}_i^* and \mathbf{v}_j^* according to the Collisional law.

- Generate two uniform random numbers ξ_1, ξ_2 .
- Set $\alpha = \text{Cos}^{-1}(2\xi_1 - 1), \beta = 2\pi\xi_2$.
- Set $\phi = (\text{Cos}\beta \text{Sin}\alpha \quad \text{Sin}\beta \text{Sin}\alpha \quad \text{Cos}\alpha)^T$.

- Set $\mathbf{v}_i^* = \frac{1}{2}(\mathbf{v}_i + \mathbf{v}_j) + \frac{1}{2}|\mathbf{v}_i - \mathbf{v}_j|\phi$,

$$\mathbf{v}_j^* = \frac{1}{2}(\mathbf{v}_i + \mathbf{v}_j) - \frac{1}{2}|\mathbf{v}_i - \mathbf{v}_j|\phi.$$

- Set $\mathbf{v}_i^{n+1} = \mathbf{v}_i^*, \mathbf{v}_j^{n+1} = \mathbf{v}_j^*$.

• else

- Set $\mathbf{v}_i^{n+1} = \mathbf{v}_i^n, \mathbf{v}_j^{n+1} = \mathbf{v}_j^n$.

- Set $\mathbf{v}_i^{n+1} = \mathbf{v}_i^n$ for the $N_i - 2N_c$ particles that have not been selected.

• End for

• Calculate macroscopic properties.

During each step, all the other $N_i - 2N_c$ particle velocities remain unchanged. Here, by $Iround(x)$, we denote a suitable integer rounding of a positive real number x .

4.2 The MDSMC Scheme (the VHS collision model molecules):

- $\Delta t = 0.5 \times 10^{-8}$ Sec

- Distribute the initial locations of the particles according to the uniform distribution.

- Given $\{\mathbf{x}_i^n, i = 1, \dots, N\}$ and $\{\mathbf{v}_i^n, i = 1, \dots, N\}$

- Set $\mathbf{x}_i^{n+1} = \mathbf{x}_i^n + \mathbf{v}_i^n \cdot \Delta t$

- for $n_i = 1$ to n_{tot}

- o Given $\{\mathbf{v}_i^n, i = 1, \dots, N\}$.

- o Define the local Knudsen number (ϵ).

- o Compute an upper bound

$\bar{\sigma} = \max[(\pi d^2 |\mathbf{v}_i - \mathbf{v}_j|)/4]$ of the cross section, $\bar{\sigma}$ is updated in each collision.

- o Set $\mu = 4\pi\bar{\sigma}$.

- o Compute

$$N_{c_i} = Iround\left(\frac{N}{2}\left(\frac{\mu\Delta t}{2\epsilon} + \frac{\mu^2(\Delta t)^2}{2\epsilon^2}\right) + \frac{N}{4}\left(\frac{\mu\Delta t}{2\epsilon}\right)\right).$$

- o Select $2N_{c_i}$ dummy collision pairs (i, j) uniformly among all possible pairs.

- o Compute the relative cross section $\sigma_{ij} = \pi d^2 |\mathbf{v}_i - \mathbf{v}_j|/4$.

- o Generate uniform random numbers ($Rand$).

- o If $Rand < \sigma_{ij}/\bar{\sigma}$

- o Perform the collision between i and j , and compute the post-collision velocities \mathbf{v}_i^* and \mathbf{v}_j^* according to the Collisional law, like the DSMC method.

- o Set $N_{c_2} = Iround\left(\frac{N}{2}\left(\frac{\mu\Delta t}{2\epsilon}\right)\right)$.

- o Select N_{c_2} particles among those that have not collided and select N_{c_2} particles among those that have collided.

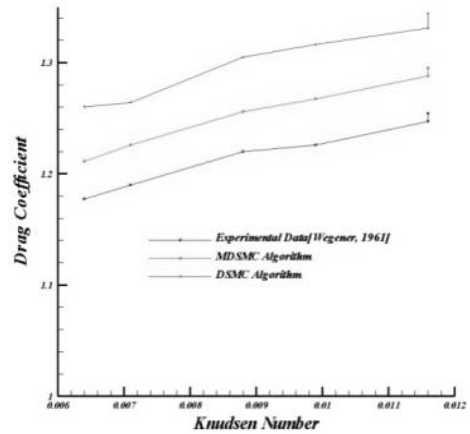


Fig. 2. The comparison of the results of simulation using the MDSMC and the DSMC schemes for the drag coefficients versus different Knudsen numbers with experimental results of Wegener, et al. (1961).

- o Compute the relative cross section $\sigma_{ij} = \pi d^2 |\mathbf{v}_i - \mathbf{v}_j|/4$.
- o Generate uniform random numbers ($Rand$).

o If $Rand < \sigma_{ij}/\bar{\sigma}$

- o Perform the collision between i and j , and compute the post-collision velocities \mathbf{v}_i^* and \mathbf{v}_j^* according to the collisional law, like the DSMC method.

- o Set $\mathbf{v}_i^{n+1} = \mathbf{v}_i^n$ for all the $N - 2N_{c_i} - N_{c_2}$ particles that

have not been selected.

• End for

• Calculate macroscopic properties.

5. Discussion of results

5.1 Comparisons of the results of simulations of gas flow about the sphere with the experiments of Wegener (1961)

Fig. 2 shows the comparison of the results of simulation using the MDSMC and the DSMC schemes for the drag coefficients versus different Knudsen numbers with experimental results of Wegener, et al. (1961). The comparison shows that the results of simulation using the MDSMC scheme for the drag coefficients are closer to the experiment (Wegener, et al. (1961)) than the DSMC scheme.

Fig. 3 shows the comparison of the results of simulation using the MDSMC and the DSMC schemes for the drag coefficients versus different Mach numbers with experimental results of Wegener, et al. (1961). The comparison shows that the results of simulation using the MDSMC scheme for the drag coefficients are closer to the experiment (Wegener, et al. (1961)) than the DSMC scheme.

Figs. 4(a) and (b) show the constant density contours using the MDSMC and the DSMC schemes, respectively.

Figs. 5a and 5b show the constant Mach number contours using the MDSMC and the DSMC schemes respectively. The contours of the constant Mach number using the MDSMC scheme are more compact than the contours of the constant Mach number using the DSMC scheme.

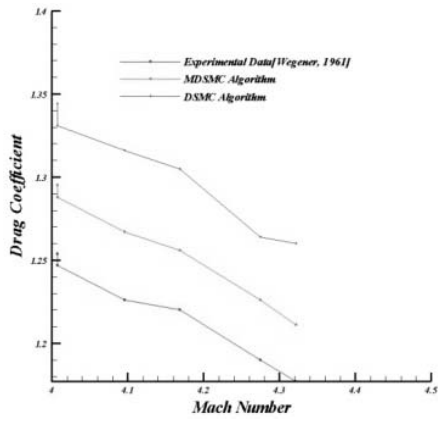


Fig. 3. The comparison of the results of simulation using the MDSMC and the DSMC schemes for the drag coefficients versus different Mach numbers with experimental results of Wegener, et al. (1961).

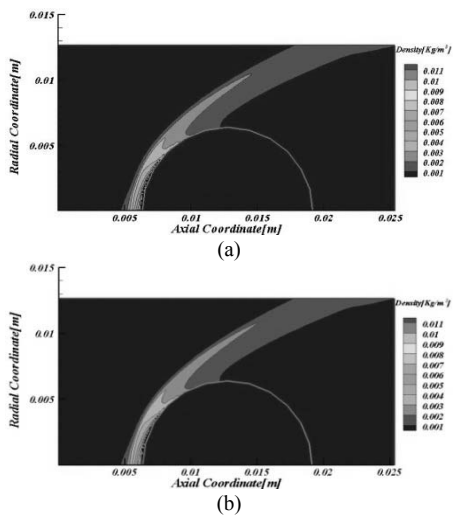


Fig. 4. The constant density contours using the MDSMC and the DSMC schemes, respectively.

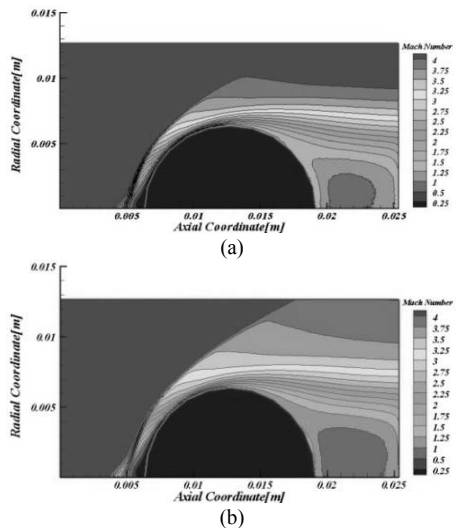


Fig. 5. The constant Mach number contours using the MDSMC and the DSMC schemes, respectively.

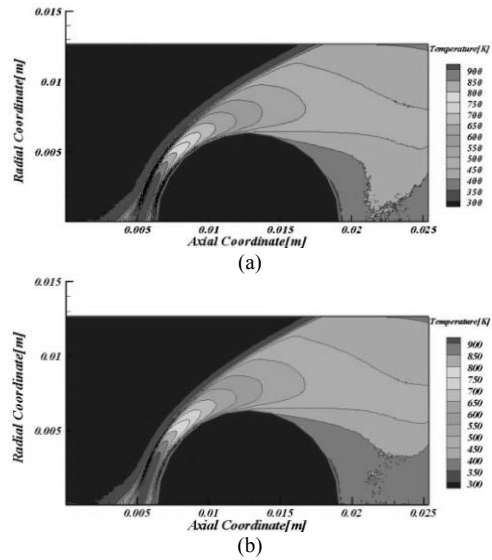


Fig. 6. The constant Temperature contours using the MDSMC and the DSMC schemes respectively.

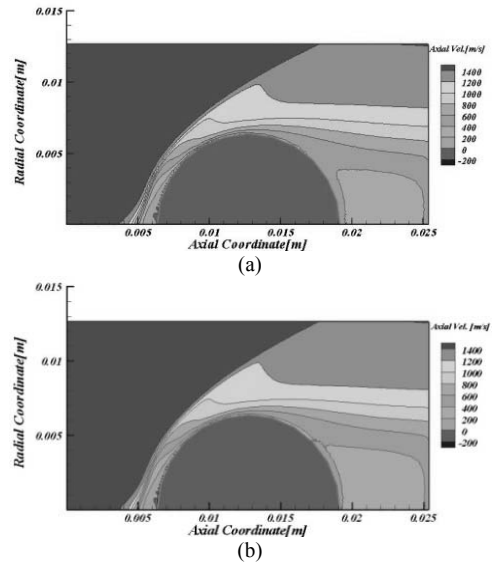


Fig. 7. The constant axial velocity contours using the MDSMC and the DSMC schemes, respectively.

Figs. 6(a) and (b) show the constant temperature contours using the MDSMC and the DSMC schemes respectively. The contours of constant temperature using the MDSMC scheme are smoother than the contours of constant temperature using the DSMC scheme in the front area of the sphere. However, the results of simulation for the constant temperature contours using the MDSMC scheme show more fluctuations in the wake zone of the sphere than the DSMC scheme.

Figs. 7(a) and (b) show the constant axial velocity contours using the MDSMC and the DSMC schemes respectively. The contours of the constant axial velocity using the MDSMC scheme are more compact than the contours of the constant axial velocity using the DSMC scheme.

Table 1. The comparison of the results of simulation for the drag coefficient of the sphere using the MDSMC and DSMC schemes with the experimental data of Wegener, et al. (1961).

Relative error of drag coefficient (the DSMC scheme)	Relative error of drag coefficient (the MDSMC scheme)	experimental data [Wegener et al, 1961]	Drag Coefficient (the DSMC scheme)	Drag Coefficient (the MDSMC scheme)	Ambient Knudsen Number	Ambient Mach Number	Ambient Temperature (K)
7.17%	3.30%	1.254	1.344	1.295	0.0116	4.007	299.65
6.74%	3.28%	1.247	1.331	1.288	0.0116	4.007	299.35
7.34%	3.34%	1.226	1.316	1.267	0.0099	4.096	299.35
6.96%	2.97%	1.220	1.305	1.256	0.0088	4.169	299.65
6.22%	3.04%	1.190	1.264	1.226	0.0071	4.275	299.25
7.05%	2.89%	1.177	1.260	1.211	0.0064	4.322	299.25

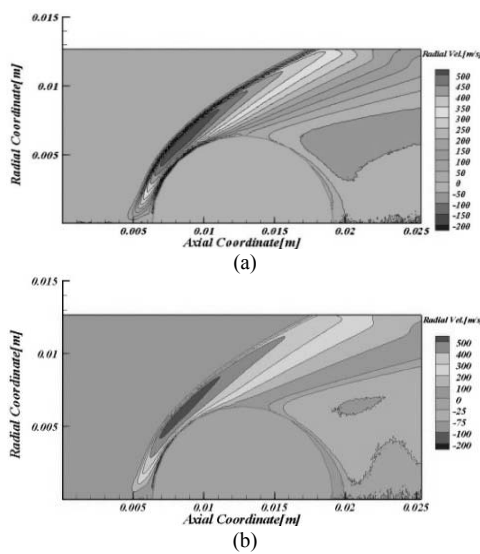


Fig. 8. The constant radial velocity contours using the MDSMC and the DSMC schemes, respectively.

Figs. 8(a) and (b) show the constant radial velocity contours using the MDSMC and the DSMC schemes, respectively. The contours of the constant radial velocity using the MDSMC scheme are more compact than the contours of the constant radial velocity using the DSMC scheme.

Table 1 shows the comparison of the results of simulation for the drag coefficient of the sphere using the MDSMC and the DSMC schemes with the experimental data of Wegener, et al. (1961). The comparison of the results of simulation for the drag coefficient of the sphere using the MDSMC and the DSMC schemes with the experimental data of Wegener, et al. (1961) shows that the error of the results for the drag coefficient of the sphere using the MDSMC scheme is 60% less than the error of the results using the DSMC scheme.

6. Conclusions

Comparing the results of the simulation with the experimen-

tal data shows that the new scheme developed in the present work (the MDSMC scheme) has the capability of simulating the rarefied gas flow problem (flow about a sphere) with higher accuracy than the previous DSMC scheme. First, in the new scheme (MDSMC) there exists a new extra term $P(f_1^n, f_2^n)/\mu$ which takes into account the effect of the collision between the particles sampled from f^n and the particles sampled from $P(f^n, f^n)/\mu$ which we call that the second-order collision term. Second, in the new scheme (MDSMC) there exists a second-order term in the time step in the probabilistic coefficients which takes into account the effect of the sampling the particles with higher accuracy than the sampling the particles in the previous DSMC scheme.

References

- [1] C. Cercignani, The Boltzmann Equation and Its Applications, Lectures Series in Mathematics, 68, Springer-Verlag, Berlin, New York (1988).
- [2] F. W. Vogenitz, G. A. Bird, J. E. Broadwell and H. Rungaldier, Theoretical and Experimental Study of Rarefied Supersonic Flows about Several Simple Shapes, *AIAA Journal*, 6 (12) (1968) 2388-2394.
- [3] G. A. Bird, Molecular Gas Dynamics and the Direct Simulation of Gas Flows, Oxford Univ. Press, London (1994).
- [4] G. A. Bird, Recent Advances and Current Challenges for DSMC, *Computers and Mathematics with Applications*, 35 (1-2) (1998) 1-14.
- [5] A. L. Garcia and F. Baras, Direct Simulation Monte Carlo: Navel Applications and New Extensions (1997).
- [6] E. Gabetta, L. Pareschi and G. Toscani, Relaxation Schemes for Nonlinear Kinetic Equation, *SIAM J. Numer. Anal.*, 34 (1997) 2168-2194.
- [7] J. F. Crifo, G. A. Lukianov, A. V. Rodionov, G. O. Khanlarov and V. V. Zakharov, Comparison Between Navier-Stokes and Direct Monte-Carlo Simulations of the Circumnuclear Coma, *Icarus* 156 (2002) 249-268.
- [8] H. Chen, S. Kandasamy, S. Orszag, R. Shock, S. Succi and V. Yakhot, Extended Boltzmann Kinetic Equation for Turbulent Flows, *Science* 301 (2003) 633-636.
- [9] J. S. Wu and Y. Y. Lian Parallel Three-Dimensional Direct Simulation Monte Carlo Method and its Applications, *Computers & Fluids* 32 (2003) 1133-1160.
- [10] J. S. Wu and K. C. Tseng, Analysis of Micro-Scale Gas Flow With Pressure Boundaries Using Direct Simulation Monte Carlo Method, *Computers and Fluids* 30 (2001) 717-735.
- [11] A. N. Volkov, Tsirkunov, M. Yu and B. Oesterle, Numerical Simulation of a Supersonic Gas-Solid Flow Over a Blunt Body: The Role of Inter-Particle Collisions and Two-Way Coupling Effects, *International J. of Multiphase Flow*, 31 (2005) 1244-1275.
- [12] S. S. Nourazar, S. M. Hosseini, A. Ramezani and H. R. Dehghanpour, Comparison between the Navier-Stokes and the Boltzmann equations for the simulation of an axially symmetric compressible flow with shock wave using the

- Monte-Carlo method, Computational Methods and Experimental Measurements XII, *WIT Transaction on Modeling and Simulation*, 41 (2005) 61-69 WIT Press.
- [13] V. K. Dogra, J. N. Moss and R. G. Wilmoth, Hypersonic Rarefied Flow Past Sphere Including Wake Structure, *J. Spacecraft Rockets*, 31 (5) (1994) 713-718.
- [14] K. Nanbu, Direct Simulation Scheme Derived From the Boltzmann Equation, *Journal of the Physical Society of Japan*, 49 (1980) 2042-2049.
- [15] H. Babovsky, On a Simulation Scheme for the Boltzmann Equation, *Mathematical Method in the Applied Sciences*, 8 (1986) 223-233.
- [16] L. Pareschi and R. E. Calfisch, An Implicit Monte-Carlo Method for Rarefied Gas Dynamics, *J. Comput. Phys.* 154 (1999) 90.
- [17] L. Pareschi and G. Russo, Time Relaxed Monte-Carlo Methods for the Boltzmann Equation, *SIAM J. Sci. Comput.* 23 (2001) 1253-1273.
- [18] L. Pareschi and S. Trazzi, Asymptotic Preserving Monte Carlo Methods for the Boltzmann Equation, *Transport Theory Statist. Phys.*, 29 (2005) 415-430.
- [19] L. Pareschi, S. Trazzi, Numerical Solution of the Boltzmann Equation by Time Relaxed Monte-Carlo (TRMC) Method, *International Journal of Numerical Method in Fluids*, 48 (2005) 947-983.
- [20] P. P. Wegener and H. Ashkenas, Wind tunnel measurements

of sphere drag at supersonic speeds and low Reynolds numbers, *Journal of Fluid Mechanics*, 10 (4) June (1961) 550-560.



S. S. Nourazar received his B.Sc. degree from Amirkabir University of Technology in Tehran, Iran. Then he continued his graduate studies in Canada and received the M. Sc. and Ph.D in Mechanical engineering from Ottawa University in Canada. Dr. Nourazar is acting now as associate professor in the Mechanical

Engineering Department of Amirkabir University of Technology. His research interests are the CFD in compressible and incompressible turbulent nonreactive flow as well as rarefied gas dynamics.



A. A. Ganjaei received his B.Sc. degree from Science & Technology of Iran University in Tehran, Iran. Then he continued his graduate studies in Amirkabir University of Technology and received the M. Sc. and PhD in Mechanical engineering. The research interests of Ganjaei are the CFD in

compressible and incompressible turbulent nonreactive flow as well as rarefied gas dynamics.